The Influence of Polar Coronal Holes on the Polar ENA Flux Observed by IBEX

Reisenfeld, Daniel Brett
Bzowski, Maciej
Funsten, Herbert O. III
Janzen, Paul H.
Karna, Nishu
Kubiak, Marzena A.
McComas, David J.
Schwadron, Nathan A.
Sokol, Justyna M.

To be published in: The Astrophysical Journal

DOI to publisher's version: 10.3847/1538-4357/ab22c0

The Influence of Polar Coronal Holes on the Polar ENA Flux Observed by IBEX

D. B. Reisenfeld[1], M. Bzowski[2], H. O. Funsten[1], P. H. Janzen[3], N. Karna[4], M. A. Kubiak[2], D. J. McComas[5], N. A. Schwadron[6], and J. M. Sokół[2]

(1)Los Alamos National Laboratory, Los Alamos, NM 87545, USA: dreisenfeld@lanl.gov; hfunsten@lanl.gov
(2) Space Research Centre of the Polish Academy of Sciences, (CBK PAN), Bartycka 18A, 00-716, Warsaw, Poland: bzowski@cbk.waw.pl; mkubiak@cbk.waw.pl; jsokol@cbk.waw.pl
(3)University of Montana, Missoula, MT 59812, USA: paul.janzen@umontana.edu
(4)Harvard-Smithsonian Center for Astrophysics, Cambridge MA 02138: nishu.karna@cfa.harvard.edu
(5)Department of Astrophysical Sciences, Princeton University, Princeton, NJ 08544, USA: dmccomas@princeton.edu
(6)University of New Hampshire, Space Science Center, Morse Hall, Durham, NH 03824, USA nschwadron@guero.sr.unh.edu

Abstract. Polar coronal holes (PCHs) fill the high-latitude heliosphere with fast solar wind during the minimum phase of the solar cycle. This leads to a hardening of the energy spectrum of the proton plasma in the inner heliosheath IHS, observed as energetic neutral atoms (ENAs) by the *Interstellar Boundary Explorer* (*IBEX*). In particular, the highest-energy channel of the IBEX-Hi instrument (at 4.3 keV) is a very sensitive indicator of pre-termination shock fast wind entering the IHS. We show that the 4.3 keV ENA flux observed from the ecliptic poles is well-correlated with the area of the solar surface covered by PCHs throughout the solar cycle, which demonstrates the existence of a direct connection between coronal structure and the dynamic properties of the IHS.

1. INTRODUCTION

Polar coronal holes (PCHs) are the sources of the fast (~760 km s^{-1}) solar wind (SW) that dominates the high-latitude heliosphere during the sunspot minimum phase of the solar cycle (McComas et al. 2000, Fujiki et al. 2005). At their maximum size, the combined area of PCHs covers only about 10% of the projected solar disk (Karna et al. 2014), or 20% of the Sun's surface area. However, due to the super-radial expansion of the polar magnetic field, PCH-associated SW is observed down to 35° latitude (McComas et al. 2000, Sokół et al. 2015, Tokumaru et al. 2017); thus, around solar minimum, PCH flow can fill 1.7π steradians, or 43% of the heliosphere. Thus, PCH SW flow will be a major component of the heliosheath plasma beyond the termination shock (TS).

The *Interstellar Boundary Explorer* (*IBEX*, McComas et al. 2009a) has observed the imprint of the fast SW from PCHs on the global heliosphere, through the observation of energetic neutral atoms (ENAs) emanating from the inner heliosheath (IHS). McComas et al. (2014) showed that the first five years of *IBEX* observations (2009 – 2013) correlates with the solar minimum phase of the solar cycle, when the travel time of outbound SW and returning ENAs (a time lag of ~4 – 2.5 years for ENAs in the range of 0.5 – 6 keV) is taken into account. During this period, a strong association was revealed between the latitudinal ordering of the ENA spectral indices and the solar minimum-like SW structure, further confirming earlier evidence of latitudinal ordering

(McComas et al. 2009b, Dayeh et al. 2011). Desai et al. (2016) predicted that the latitudinal ordering of the spectral indices would be disrupted in the 2014-2017 timeframe as the ENA signal began to reflect the increase in solar activity and the closing of the PCHs that was observed at the Sun beginning in 2011. This was also predicted by McComas et al. (2012, 2014) and later confirmed by McComas et al. (2017a). Recently, Zirnstein et al. (2017) showed that the spectral index of the ENA energy distribution measured at a particular time in a particular direction is correlated with the speed of the outgoing SW traveling in that direction, adjusted for the travel time.

The link between the ENA energy distribution and the SW speed is not necessarily obvious, because the SW undergoes significant processing as it propagates through the heliosphere. The supersonic SW flows radially away from the Sun and interacts with interstellar atoms, ionizing many of them via charge exchange. Once ionized, the interstellar ions are accelerated ("picked up") by the SW magnetic field (e.g., see McComas et al. 2017b for PUI observations in the SW out to ~38 AU). The SW is in turn mass-loaded and slowed as it approaches the TS (Richardson et al. 2008, Lee et al. 2009). As the supersonic SW and its pickup ion (PUI) component cross the TS at > 80 au from the Sun, they become subsonic, compressed, and heated in the IHS. In fact, the effect of the TS passage on the flow is to transfer 80% or more of the flow energy into the PUIs (Richardson et al. 2008).

In the heliosheath, the particle distribution is no longer Maxwellian and is better represented by a Kappa distribution (e.g. Zank et al. 2010; Livadiotis et al. 2011), with the PUI portion of the distribution described by a power law. ENAs are formed when interstellar atoms flowing into the heliosphere charge-exchange with the energetic protons of the heliosheath. These ENAs travel ballistically from their point of origin in all directions. Some of them travel toward Earth and are detectable by *IBEX*.

Zirnstein et al. (2017) quantified the latitudinal evolution of the ENA spectra over time, and the relationship of the spectra to the evolution of the SW. In addition, Reisenfeld et al. (2016, hereafter R2016) used 7 years of IBEX observations to show that the polar ENA flux correlates well with the phase of the solar cycle, and that the continuing decrease of the high energy ENA fluxes through 2015 was consistent with the disappearance of the fast SW earlier in the solar activity cycle.

Beginning in 2014, the Sun's PCHs began to reopen. R2016 therefore predicted that within a few years, the high energy polar ENA flux would begin to recover. In this paper, we investigate whether this has come to pass. Here, we report the most recent polar ENA flux observations, and look more deeply into their relation with the size of the Sun's PCHs.

2. OBSERVATIONS

We use IBEX-Hi ENA observations of the ecliptic poles spanning the first 9.5 years of the mission (25 December 2008 – 25 June 2018), covering the full period of IBEX-Hi validated data to date (McComas et al. 2019). *IBEX* is a sun-pointing spinning spacecraft equipped with two instruments, IBEX-Lo, which images ENAs from ~10 eV – 2 keV (Fuselier et al. 2009), and IBEX-Hi, which images ENAs from ~0.5 – 6 keV (Funsten et al. 2009). As with previous polar studies (Reisenfeld et al. 2012; R2016) we take advantage of the fact that the IBEX sensors view the ecliptic poles once every spin. This allows for both higher time resolution observations and much higher counting statistics than for observations of other parts of the sky. The ecliptic pole analysis method follows that described in R2016. All data are corrected for spacecraft aberration and for backgrounds (see McComas et al. 2017a). The ENA flux measurements are also adjusted for the survival probability of ENAs travelling 100 AU from beyond the TS to 1 au (Bzowski 2008; McComas et al. 2017a) so that they reflect the expected ENA flux in the heliosheath.

In addition to ENA observations from *IBEX*, we make use of EUV observations of the solar disk from a combination of Extreme-ultraviolet Imaging Telescope (EIT) synoptic maps from the *Solar and Heliospheric Observatory* (*SoHO*) and Atmospheric Imager Assembly (AIA) synoptic maps from the *Solar Dynamics Observatory* (*SDO*). These were analyzed to determine the fraction of the solar disk covered by PCHs as a function of Carrington Rotation (the 27.27-day rotation period of a sunspot), applying the method of Karna et al. (2014).

3. ANALYSIS

Our goal is to analyze, by as direct a means as possible, the relationship between the configuration of the high-latitude solar corona and the structure of the IHS. We compare the area of the solar disk covered by the PCH of a given pole to the magnitude of the ENA flux measured in the direction of the corresponding ecliptic pole by the highest IBEX-Hi energy channel, which is centered at 4.3 keV. The link between the PCH area and the 4.3 keV ENA flux is the high-speed SW that emanates from the PCHs. Of the six IBEX-Hi energy channels, the 4.3 keV channel is the most sensitive to fast SW speed. Zirnstein et al. (2017) demonstrated that 450 km s^{-1} SW yields an ENA energy power law with a spectral index of $\gamma \sim 2.2$, and that 750 km s^{-1} SW yields $\gamma \sim 1.3$. Assuming equal total flux over the measured IBEX-Hi energy range, this corresponds to a factor three greater flux in the 4.3 keV channel for 750 km s^{-1} wind than for 450 km s^{-1} wind. Thus, by monitoring the polar 4.3 keV ENA flux over time, we can determine how much of the IHS over the pole is filled with plasma originating from the fast wind.

In comparing the polar ENA flux to the area of a PCH, the question then becomes which ENA flux interval to choose for comparison. There is a time delay of two to four years between the outgoing SW and the returning ENA flux. We therefore have to determine the appropriate time delay in order to select the corresponding *IBEX* measurement interval. To determine the time offset, or the "trace-back" time t_{tb}, we time-correlate the SW dynamic pressure of the outgoing SW measured in the ecliptic at 1 au with the ENA-derived IHS plasma pressure measured by IBEX-Hi. The rationale for this method is that the plasma pressure in the IHS will respond to changes in the SW dynamic pressure incident on the TS, and the ENA flux emitted from the IHS will be proportional to this time-varying IHS plasma pressure. Use of the SW dynamic pressure measured in the ecliptic is valid for analysis of the poles because the SW dynamic pressure is latitude invariant on the time scales relevant here (McComas et al. 2008).

The method for finding t_{tb}, described in detail in R2016, involves estimating the distance to the TS (d_{TS}) and thickness of the IHS (l_{IHS}) to come up with a value for t_{tb}, and then iteratively adjusting these distances until the best pressure correlation is found. We have since made two improvements to the procedure. First, we have modified the definition of t_{tb} to reflect the findings of McComas et al. (2018) and Zirnstein et al. (2018). Specifically, Zirnstein et al. (2018) simulated a SW dynamic pressure pulse incident on the TS and then examined the evolution of this pulse as it propagates through the heliosheath, causing a corresponding increase in the heliosheath pressure and rise in the ENA flux intensity. They found that to properly determine the time it takes for the IHS to respond to the pulse, one must allow the pulse to propagate completely through the heliosheath and reflect off the heliopause. Only after the pulse rebounds does the plasma pressure fully adjust to a change in the SW dynamic pressure. Thus, we now use Equation (2) of Zirnstein et al. (2018) to calculate t_{tb}.

The second modification is the method for choosing the speed for the outgoing SW, v_{SW} . R2016 used a constant speed of 755 km s^{-1}, based on PCH wind speeds observed by Ulysses during solar minimum (McComas et al. 2000). In this work, the period of observation is a full solar cycle (from minimum in 2009 through maximum in 2014 to minimum in 2018) and we need to account for the cyclic changes of the polar SW speed, which can drop as low as ~ 450 km s^{-1} at solar maximum (e.g. Ebert et al. 2009, Tokumaru et al. 2015). We therefore use the high-latitude time-dependent SW speeds reported by Sokół et al. (2015) derived from interplanetary scintillation observations (Tokumaru et al. 2012). Note that, as in R2016, we reduce the outgoing SW speed by 10% from these observed values to account for the decrease in SW speed due mass loading by PUIs.

With this modified form of the R2016 procedure, we have derived t_{tb} for all polar ENA observations for the first 9.5 years of the *IBEX* mission. As this method does not uniquely fix both d_{TS} and l_{IHS}, we choose values for $d_{TS} = 110$ au for the north pole and 100 au for the south, based on the *Voyager* TS crossing distances (Stone et al. 2005, Richardson et al. 2008) and the knowledge that the TS has a north-south asymmetry, as determined from both *Voyager* and from *IBEX* ENA observations (McComas et al. 2018, 2019). We then vary l_{IHS} to find the best pressure correlation, arriving at a value of $l_{IHS} = 50$ au for both north and south poles.

It follows that the trace-back time for 4.3 keV ENAs averages to 3.0 ± 0.6 years for the north pole, and slightly less, 2.7 ± 0.6 years for the south, the range being due to the variation in SW speed observations. We apply these time shifts to the IBEX 4.3 keV north and south ecliptic pole ENA time series, and compare them with the areas of the north and south PCHs.

Figure 1 shows this comparison. Plotted are monthly averages of the 4.3 keV ENA flux from the ecliptic poles, and the corresponding PCH areas. For the overlap period between 2006 and 2015 (corresponding to the declining phase of SC23 and the ascending phase of SC24), the time-shifted ENA flux and the PCH areas show a striking degree of correlation. We emphasize that the time shifts of the north and south pole ENA fluxes were determined by applying the pressure correlation method to *in ecliptic* SW observations, and yet this results in an excellent match between the time series of the 4.3 keV ENA flux and the PCH area at each pole, respectively.

As good as the correlation is, there are a couple of differences to point out. In the north (Figure 1a), there is a noticeable lag, of almost 2 years, between the closure of the PCH and the decline of the ENA flux to its minimum value. In the south (Figure 1b), although the lag is not as significant, the ENA flux minimum is considerably less deep than the PCH area minimum, nor as deep as the ENA flux minimum in the north.

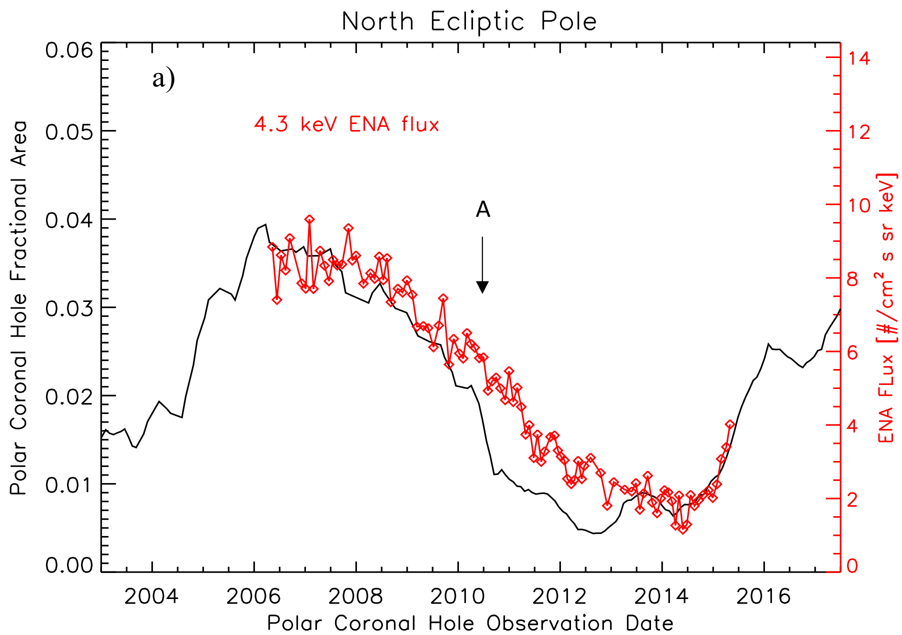

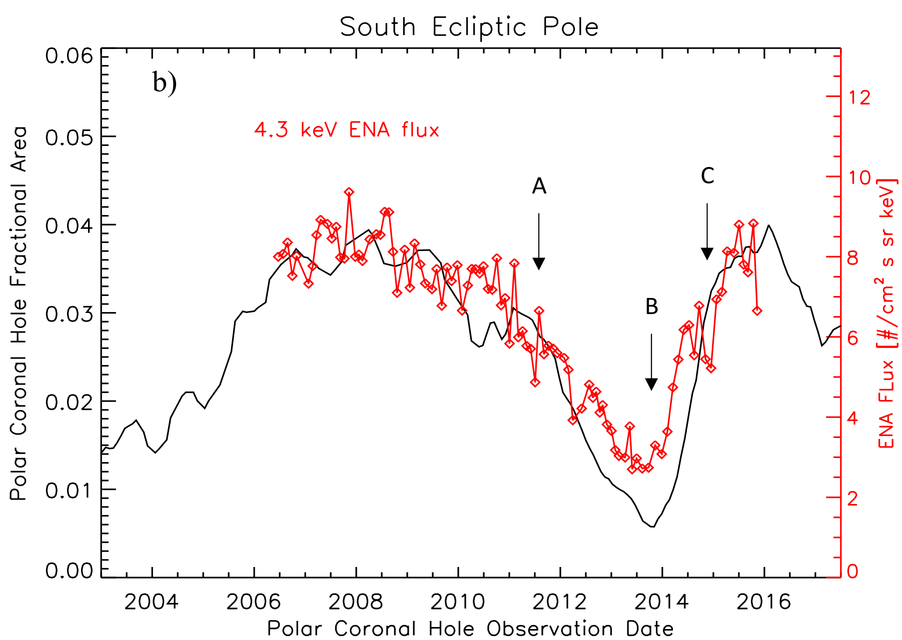

Figure 1. *Comparison of the time-shifted IBEX-Hi 4.3 keV ENA flux (red) with the fractional area (black) of the PCH for the (a) north and (b) south ecliptic poles. Arrow 'A' marks the time depicted in Figure 2, and arrow 'B' the time depicted in Figure 3. Arrow 'C' marks the approximate arrival time of the ENA pressure enhancement described in McComas et al. (2019) near the south pole. The PCH data have been smoothed with a 12-Carrington Rotation running average to eliminate the periodicity introduced by the ±7° annual excursion of the Earth in heliolatitude.*

We mention that McComas et al. (2018) report that a strong increase in the SW dynamic pressure observed at 1 au in the second half of 2014 generated a 4.3 keV ENA enhancement first detected at *IBEX* from a direction ~20° south of the heliospheric nose in late 2016. This enhancement has steadily grown in area, and by mid-2017, it has extended down close to the south pole (McComas et al. 2019). We observe a mild rise in the ENA flux at this time (arrow 'C' in Figure 1b); thus, it appears that the ENA enhancement has merged with the increasing ENA flux from the opening of the PCH. Note that the shallowness of the ENA flux minimum in the south (arrow 'B') is not associated with the pressure enhancement, as the minimum is observed well before effects of the enhancement would be observed. Finally, we note that as of mid-2018, the enhancement has yet to reach the north pole, thus the rise in ENA flux we see there is due entirely to the opening of the PCH.

4. DISCUSSION

We propose the following explanation for why the area of the solar surface covered by PCHs and the 4.3 keV polar ENA flux emanating from the distant heliosheath are so well correlated.

Consider the flux of ENAs incident on IBEX from a particular look direction. The line-of-sight (LOS) in this direction intercepts a collection of IHS streamlines that can be traced to solar wind originally propagating outward from the Sun along radials arranged between the pressure maximum in the heliosheath (located 20° south of the nose; McComas & Schwadron 2014) and the look direction of IBEX. The ENA flux should correlate in some manner with the properties of the outbound solar wind averaged over these radial directions.

In the case of ENA observations along a given ecliptic pole, in principle the ENA flux should reflect the properties of the SW flux averaged over all latitudes from the heliosheath pressure maximum to the pole, and over a narrow wedge of longitudes centered on the upwind direction. In actuality, the ENAs observed at the poles will be affected by SW flux over a more limited range of latitudes due to the finite lifetime of protons arcing along streamlines in the heliosheath. Since we are concerned here with ENAs arising from protons with an energy ~ 4 keV, a charge-exchange calculation assuming a neutral density of $n_H = 0.1 \text{ cm}^{-3}$ gives a lifetime for such protons of ~3 years before they are neutralized. These protons will be tied to a bulk plasma distribution that has a flow speed somewhere between 150 km s^{-1} and 250 km s^{-1}, corresponding to pre-TS SW with a speed between 400 km s^{-1} and 700 km s^{-1}. Taking the average, 200 km s^{-1}, the typical distance heliosheath plasma will flow in 3 years is 125 au. Then assuming an average distance from the Sun to the mid-point of the IHS of ~120 au, this corresponds to an arc of approximately 55º. Therefore, we expect the 4.3 keV ENAs observed at the poles to be emitted by a sample of processed SW protons originating from heliolatitudes above 35º. Interestingly, this turns out to cover the maximum latitudinal extent of the fast SW from PCHs at solar minimum (McComas et al., 2000). At any other time during the solar cycle, the range of latitudes filled by PCH SW will be less. Since we have already established that 4.3 keV ENAs are strongly associated with the fast SW, it follows that the magnitude of the polar 4.3 keV ENA flux will be proportional to the size of the PCH.

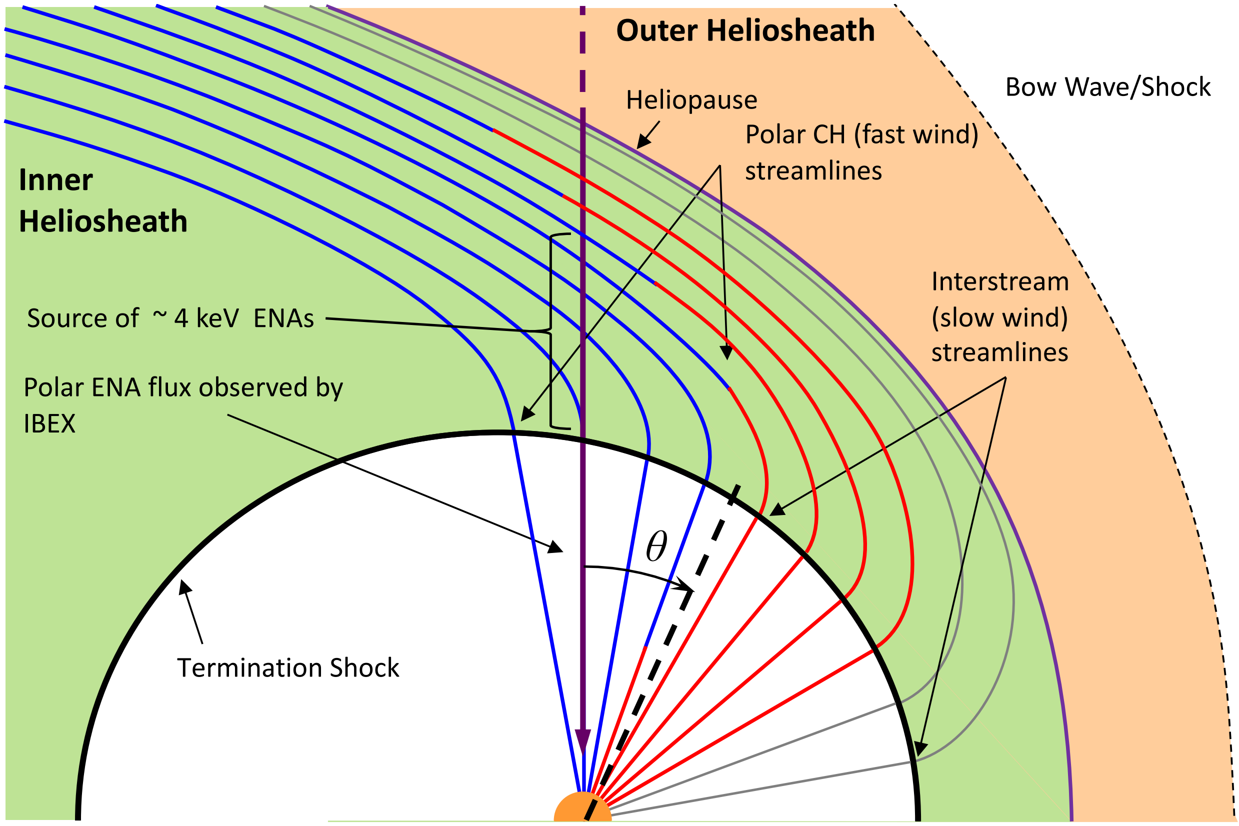

Figure 2. *A schematic meridional snapshot of the heliosphere during the ascending phase of the sunspot cycle, when the PCH is decreasing in size. Blue streamlines represent the fast SW PCH flow, red streamlines represent the slow SW. Grey streamlines represent low-latitude SW that is depleted in ~ 4 keV protons by the time it reaches the pole. Thus, they do not contribute to the 4.3 keV ENA signal. The angle θ is the opening angle of the cone containing PCH flow (fast SW) arriving at the TS. Note that although only the northern heliosphere is shown here, this represents the situation for either hemisphere. See text for discussion.*

We now look in detail at the phasing between the PCH size and the 4.3 keV ENA flux. Figure 2 depicts a schematic meridional cut through the heliosphere showing its configuration during the ascending phase of the solar cycle when the PCH is shrinking (arrow 'A' in Figures 1a and 1b). Shown are streamlines representing the SW traveling out from the Sun at a range of latitudes, crossing the TS, and then being deflected poleward. Blue streamlines represent the fast polar wind, and red streamlines represent the slow interstream wind. The angle θ defines the opening angle of the cone containing PCH flow (blue streamlines) arriving at the TS. Grey streamlines represent wind from latitudes below 35° that contribute negligibly to the polar 4.3 keV ENA signal due to charge exchange loss. The vertical line along the pole is the *IBEX* LOS of interest here. The magnitude of the observed 4.3 keV flux will be proportional to the fraction of blue vs. red streamlines the LOS intercepts. At solar minimum when the PCH is at maximum size, all of the colored (non-grey) lines would be blue. After solar minimum, the mid-latitude streamlines will turn red as the heliosphere re-fills with slow SW (as depicted in Figure 2), and thus the 4.3 keV ENA flux will begin to decrease. Note that at the instant depicted here, the fraction of latitudes filled by the slow wind upstream of the TS is much larger than the fraction of slow versus fast wind intercepted by the LOS, due to finite travel time of plasma along the streamlines. This results in a larger phase lag between closure of the PCH and the drop in 4.3 keV flux than what can be attributed to the trace-back time (seen most prominently for the north PCH in Figure 1a).

We turn next to Figure 3 which represents a snapshot of the heliosphere just after solar maximum, as a new PCH begins to form (arrow 'B' in Figure 1b). Right at the point where the PCH is completely closed (just prior to the situation shown in Figure 3), all streamlines leaving the Sun will carry slow SW (red). However, the polar LOS will still intercept some fast IHS flow (blue). This is due to the fact that the rate at which the PCH closes is faster than the rate at which fast IHS flow can move out of the south pole LOS.

We can confirm this quantitatively by referring to Figure 1b and calculating the closure rate of the south PCH between points A (at year 2011.5) and B (at year 2013.8) and comparing this to the flow speed in the IHS. As noted above, when the PCH is fully open, coronal hole flow in the heliosphere extends equatorward to about latitude 35°S. By treating the PCH area as a proxy for the latitude of the opening angle θ of the cone containing coronal hole flow, it follows that point A corresponds to $\theta = 45°$S. Likewise, to within the uncertainty of the PCH fractional area determination (±0.005, Karna et al. 2014), point B corresponds to full closure of the PCH. The closure rate is then about 20° yr^{-1}, or, projecting the coronal hole flow cone out to the TS at ~100 au, the point where the cone intersects the TS is travelling southward along the TS surface at an average speed of ~160 km s^{-1}. This is likely an underestimate of the speed when the edge reaches high latitudes ($\theta \gtrsim 60°$S), as the angular closure rate will accelerate even if the area decreases linearly due to the non-linear relationship between area and opening angle.

Turning to the flow in the IHS, the speed of the fast/slow (blue/red) boundary travelling along a streamline will be about 200 km s^{-1} (taking the average of the fast and slow IHS plasma speeds discussed above). Referencing Figure 3, at high latitudes, the average radial flow component along a streamline is equal or greater than the transverse flow component. Although this is only a schematic representation of the heliosheath, the notion that near solar maximum the polar IHS flow is more radial than not is supported by MHD simulation (see, e.g., Figure 4, Zirnstein et al. 2017). Taking the average flow angle in the high-latitude IHS to be $\lesssim 45°$ from the radial, the transverse velocity component will then be $\leq 200 \sin 45° = 140$ km s^{-1}. Thus, we see that the closure rate of the edge of the coronal hole flow cone (> 160 km s^{-1}) is greater than the rate at which fast IHS plasma passes out of the polar LOS. Therefore, the LOS along the south pole will intercept fast IHS plasma for some time after the PCH closes.

As the PCH begins to reopen, something interesting happens: If the PCH remains closed for only a brief period of time, as it does in the south (Figure 1b), the polar LOS may intercept fast IHS flow from both the tail end of the previous PCH and the new PCH at the same time. This situation is depicted in Figure 3. Thus, the minimum in the 4.3 keV ENA signal will not be as deep as the minimum in the PCH area since the LOS is still intercepting plasma associated with the previous PCH. The situation in the north (Figure 1a) is different because the north PCH stays closed for a longer period and fast wind from the previous PCH can all move beyond the north-pole LOS before the PCH begins to reopen, causing a deeper drop in 4.3 keV flux.

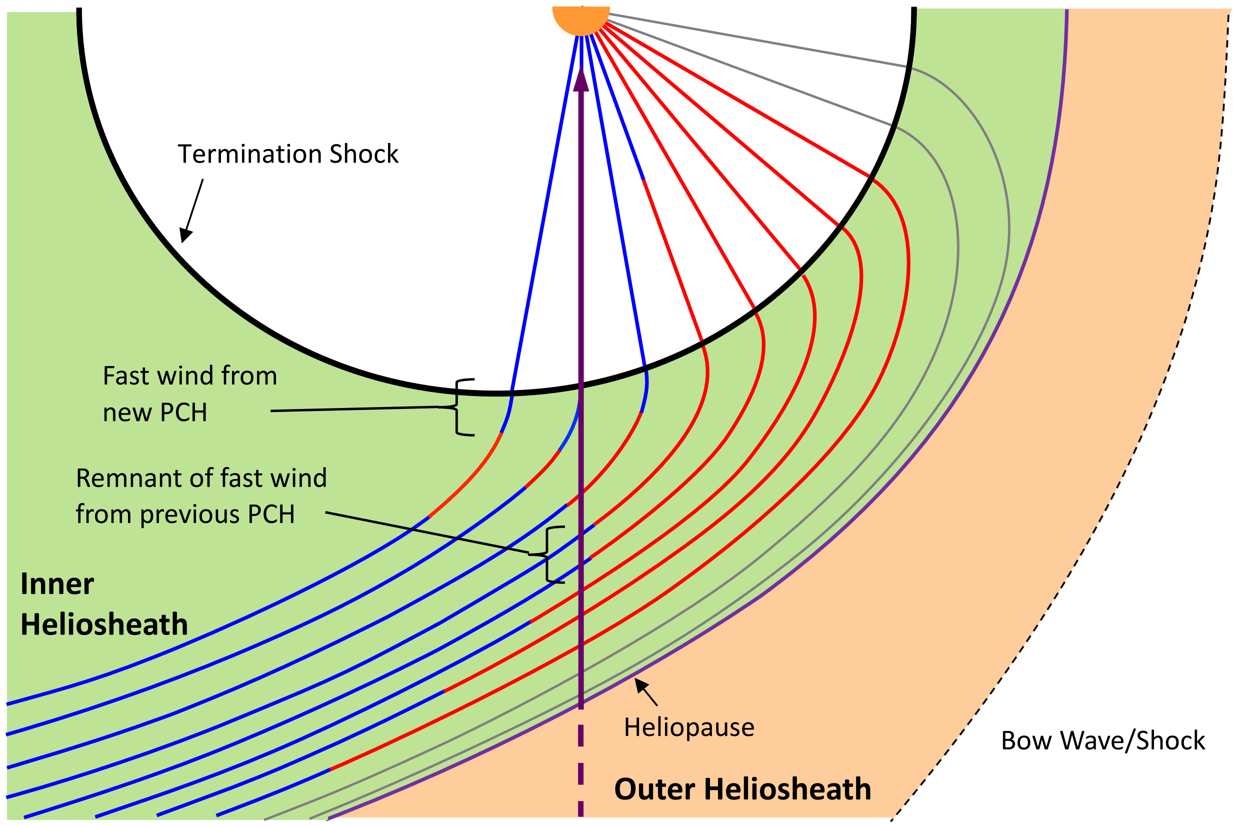

Figure 3. *Same as Figure 2, except for the southern hemisphere of the heliosphere just after solar maximum when the PCH begins to re-open. See text for discussion.*

What we depict here is a qualitative scenario, presented as a reasonable explanation for the key aspects of the observations. To more accurately test and validate this scenario, time-dependent global heliospheric modelling is required that includes realistic initial conditions representing the evolution of the global SW through the solar cycle. Nevertheless, we argue that the strong correlation between PCH area and 4.3 keV ENA flux gives unambiguous evidence that the dynamics of the heliosheath are directly related to the structure of the solar corona in a straightforward manner. We look forward to the next 2-3 years of IBEX observations as a complete solar cycle of measurements is completed, and we anticipate the full return of the north 4.3 keV ENA flux in response to the reopening of the north PCH.

This work was carried out as part of NASA's *IBEX* Mission, with support from NASA's Explorer Program (NNG17FC93C; NNX17AB04G). M.B., M.A.K., and J.M.S. acknowledge the support by the grant 2015-18-M-ST9-00036 from the National Science Center, Poland.

References:

Bzowski, M. 2008, A&A, 488, 1057
Dayeh, M. A., McComas, D. J., Livadiotis, G., et al. 2011, ApJ, 734, 29
Desai, M. I., Dayeh, M. A., Allegrini, F., et al. 2016, ApJ, 832, 116
Ebert, R. W., McComas, D. J., Elliott, H. A., et al. 2009, JGR, 114, A01109

Fujiki, K., Hirano, M., Kojima, et al. 2005, Adv.Sp.Res., 35, 2185
Funsten, H. O., Allegrini, F., Bochsler, P., et al. 2009, SSRv, 146, 75
Fuselier, S. A., Bochsler, P., Chornay, D., et al. 2009, SSRv, 146, 117
Karna, N., Hess Webber, S. A., & Pesnell, W. D. 2014, SoPh, 289, 3381
Lee, M.A., Fahr, H.J., Kucharek, H., et al. 2009, SSRv 146, 275
McComas, D. J., Barraclough, B. L., Funsten, H. O., et al. 2000, JGR, 105, 10,419
McComas, D.J., Ebert, R.W., Elliott, H.A., et al. 2008, GRL 35, L18103
McComas, D. J., Allegrini, F., Bochsler P., et al. 2009a, SSRv,146, 11
McComas, D. J., et al. 2009b, Science, 326, 959
McComas, D. J., Dayeh, M. A., Allegrini, F., et al. 2012, ApJS, 203, 1
McComas, D. J., Allegrini, F., Bzowski, M., et al. 2014, ApJS, 213, 20
McComas, D. J. and Schwadron, N. A. 2014, ApJL, 795, L17
McComas, D. J., Zirnstein, E. J., Bzowski, M., et al. 2017a, ApJS, 229, 41
McComas, D. J., Zirnstein, E. J., Bzowski, M., et al. 2017b, ApJ, 233, 8
McComas, D. J., Dayeh, M. A., Funsten, H. O., et al. 2018, ApJL, 856, L10
McComas, D. J., Dayeh, M. A., Funsten, H. O., et al. 2019, ApJ, 872, 127
Reisenfeld, D. B., Allegrini, F., Bzowski, M., et al. 2012, ApJ, 747, 110
Reisenfeld, D. B., Bzowski, M., Funsten, H. O., et al. 2016, ApJ, 833, 277
Richardson, J. D., Kasper, J. C., Wang, C., et al. 2008, Nature, 454, 63
Sokół, J. M., Swaczyna, P., Bzowski, M., et al. 2015 SoPh, 290, 2589
Stone, E. C., Cummings, A. C., McDonald, F. B., et al. 2005, Sci, 309, 2017
Tokumaru, M., Kojima, M., & Fujiki, K. 2012, JGR 117, A06108
Tokumaru, M., Fujiki, K., & Iju, T. 2015, JGR 120, 3283
Tokumaru, M., Satonaka, D., Fujiki, K., et al. 2017, SoPh, 292, 41
Zank, G. P., Heerikhuisen, J., Pogorelov, N. V., et al. 2010, ApJ, 708, 1092
Zirnstein, E. J., Dayeh, M. A., McComas, D. J., & Sokół, J. M. 2017, ApJ, 846, 63
Zirnstein, E. J., Heerikhuisen, J., McComas, D. J., et al. 2018, ApJ, 859, 104